Journal of Alloys and Compounds 509 (2011) 6447–6451

Contents lists available at ScienceDirect

Journal of Alloys and Compounds

journal homepage: www.elsevier.com/locate/jallcom

Charge ordering analysis by electrical and dielectric measurements in $Ca_{2-x}Pr_xMnO_4$ ($x = 0$–0.2) compounds

M.T. Tlili[a,*], N. Chihaoui[a], M. Bejar[a], E. Dhahri[a], M.A. Valente[b], E.K. Hlil[c]

[a] Laboratoire de Physique Appliquée, Faculté des Sciences, Université de Sfax, 300 Sfax, Tunisia
[b] I3N and Physics Department, University of Aveiro, 3810-193 Aveiro, Portugal
[c] Institut Néel, CNRS, Université J. Fourier, BP 166, 38042 Grenoble, France

ARTICLE INFO

Article history:
Received 11 November 2010
Received in revised form 12 March 2011
Accepted 15 March 2011
Available online 22 March 2011

Keywords:
Ruddlesden–Popper manganites
Charge-ordering
Dielectric permittivity
Impedance
Activation energy

ABSTRACT

$Ca_{2-x}Pr_xMnO_4$ ($0 \le x \le 0.2$) polycrystalline ceramic powders were synthesized by sol–gel method. The X-ray diffraction (XRD) profiles were indexed with a tetragonal and orthorhombic structure for Ca_2MnO_4 and Pr-doped compounds, respectively. Electrical properties were investigated by dc and ac electrical measurements. The dc measurements have revealed an insulating state for all compounds in 80–350 K temperature range. Both dc and ac measurements have highlighted a charge ordering (CO) transition at $T_{CO} = 233$ and 245 K for $x = 0.175$ and 0.2, respectively. The CO state was found to be accompanied by a jump of the hopping activation energy and a rapid rise of both dielectric permittivity and imaginary part of ac electrical impedance.

1. Introduction

The interest in materials with perovskite structure is explained by their potential technological applications arising from their various and interesting physical properties [1–3]. The Mn-based perovskite oxides have been a renewed subject of numerous investigations in recent years [4–7], because of their colossal magnetoresistance and giant volume magnetostriction near room temperature, required by the technology of various sensors and magnetomechanical devices.

The calcium-doped rare earth manganites with the formula $Ln_{1-x}Ca_xMnO_3$, where Ln = La, Pr or Nd, show a variety of electronic and magnetic properties, which result in an asymmetry between the electron and hole-doped regions. For Mn^{3+} concentrations, the two sublattices (Mn^{3+} and Mn^{4+}) become ordered and the electrons become localized, leading to a charge-ordering state (CO) with an associated antiferromagnetic (AF) behavior [8]. The CO state is related to the weakening of double-exchange (DE) mechanism within ferromagnetic (FM) clusters, explained by the interruption of Mn^{3+}–O–Mn^{4+} bond [2]. The CO property is not only limited to manganites [9,10]; but also other materials exhibit this property as well, as observed in $NdBaFe_2O_5$ [11] and $La_{1/3}Sr_{2/3}Fe_{1-x}Cr_xO_3$ [12] compounds. Moreover, it has been discovered that the CO process is accompanied by an increase of the dielectric properties [13,14] and is particularly reported that $Pr_{0.65}Ca_{0.28}Sr_{0.07}MnO_3$ single crystal has high capacitive behavior just below $T_{CO} = 250$ K (T_{CO}: CO temperature) [15]. Polycrystalline $La_{1.5}Sr_{0.5}NiO_4$ [16], $CaMn_7O_{12}$ [17,18] and thin films $La_{1-x}Ca_xMnO_3$ [19,20] also have showed high values of the dielectric constant (ε_r) attributed to the important role of CO state. The Ruddlesden–Popper (RP) manganites (Ln, A)$_{n+1}Mn_nO_{3n+1}$, which consist in a regular intergrowth of single rock-salt with multiple perovskite layers [21], display interesting magnetic, electrical and CO properties depending on material-doping. The $Ca_{2-x}Ln_xMnO_4$ compounds (Ln = Pr, Sm, Gd, Ho), exhibiting a classical K_2NiF_4-type structure, are good examples of RP manganites and are a subject of diverse magnetic, electric, dielectric, and charge-ordering studies. For Ln = Pr, dielectric characterisation of Mn^{3+}/Mn^{4+} mixed oxides $Ca_{2-x}Pr_xMnO_4$ ($x = 0.25$, 0.33 and 0.50) shows a CO transition at T_{CO} depending on x-value [22].

In this paper, we report the Pr-doping effects on electrical and dielectric properties, in order to study the CO behavior in $Ca_{2-x}Pr_xMnO_4$ compounds with a large doping range; $x = 0.05$, 0.125, 0.15, 0.175 and 0.2. The experimental study of dc resistivity, ac impedance and dielectric permittivity, versus temperature and composition, is reported.

2. Experimental

Polycrystalline $Ca_{2-x}Pr_xMnO_4$ compounds ($x = 0$–0.2) were prepared via sol–gel reaction by mixing high purity materials: $Ca(NO_3)_24H_2O$ (98%), MnO_6 (99%) and

* Corresponding author. Tel.: +216 97094554; fax: +216 74676609.
E-mail address: medtahar59@yahoo.fr (M.T. Tlili).

0925-8388/$ – see front matter © 2011 Elsevier B.V. All rights reserved.
doi:10.1016/j.jallcom.2011.03.088

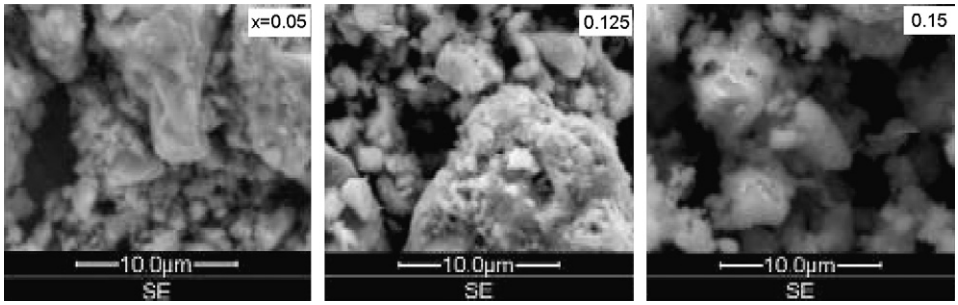

Fig. 1. SEM micrographs of $Ca_{2-x}Pr_xMnO_4$ ($x = 0.05$, 0.125 and 0.15) compounds.

Pr_6O_{11} (99.9%). The products were dissolved in diluted HNO_3 (30%). After addition of citric acid solution and ethylene glycol (4 g of citric acid/1 ml of ethylene glycol), the samples were heated until the formation of brown gel and subjected to six cycles of sintering at 500 °C, 900 °C, 1000 °C, 1100 °C and 1200 °C for 48 h and a last cycle at 900 °C for two weeks. Samples were grinded and pressed with less than 2 tonnes, into a disc shape of 8 mm diameter for every cycle. The structure was characterized at room temperature by X-ray powder diffractometer (Siemens D5000) with CuKα radiations (λ = 1.54056 Å) by scanning step (0.02°) in the range $10° \leq 2\theta \leq 90°$ and a counting time of 18 s per step. The phase analysis was carried out using FULLPROF program based on the Rietveld method.

To ensure good electrical contact with the electrodes, the opposite sides of samples (discs of 8 mm diameter and 1–2 mm thickness) were painted with silver paste. The dc electrical conductivity was measured with a Keithley electrometer, model 617, in temperature range from 80 to 400 K. The ac dielectric measurements were carried out using a parallel-plate capacitor coupled to a precision LCR meter Agilent 4284 able to measure in 20 Hz–1 MHz frequency range. The capacitor was mounted in an aluminum box refrigerated with liquid nitrogen, and incorporating a mechanism to control the temperature from 80 to 350 K.

3. Results and discussion

3.1. Structural properties

The X-ray diffraction (XRD) spectra at room temperature had been published in our previous work [23]. We have found that all samples are single phase with a perovskite-related K_2NiF_4 structure. Fig. 1 shows SEM micrographs for three samples. The nature, shape and distribution of grains suggest that all compounds have polycrystalline characteristics. Some agglomerations are shown on each pellet surface. The micrographs show an increase of grains size with the Pr-content. The XRD profiles were indexed with a tetragonal (tetra) ($I4_1/acd$) structure for Ca_2MnO_4 and orthorhombic (ortho) (Aba2) one for Pr-doped compounds. Fig. 2 shows an example ($x = 0$) of refinement result. From Fig. 3, we can remark the appearance of doublets peaks with a large spectra change just after the first Pr-doping ($x = 0.05$) highlighting a tetra–ortho structural transition. This transition is the result of the distortion of the MnO_6 octahedra around c-axis [24]. According to the literature [24,25], for several rare earth doping elements (Ln = Sm, Sr, Nd, Ho, Lu, Y.), $Ca_{2-x}Ln_xMnO_4$ compounds preserve the tetragonal structure for a wide x-composition range. The results of the Rietveld refinement are shown in Table 1. The tetra–ortho structural transition (Fig. 4) was found to be accompanied by an increase of the a parameter and a decrease of the c parameter and the cell volume (V). In the

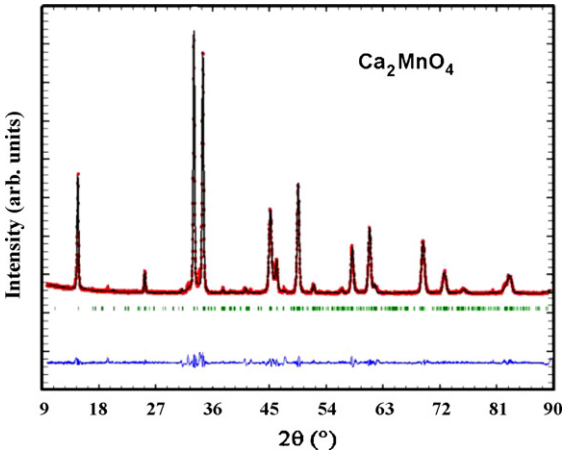

Fig. 2. Observed (solid circles) and calculated (solid line) XRD patterns of Ca_2MnO_4 compound at room temperature. The difference between these spectra is plotted at the bottom. Bragg reflections are indicated by ticks.

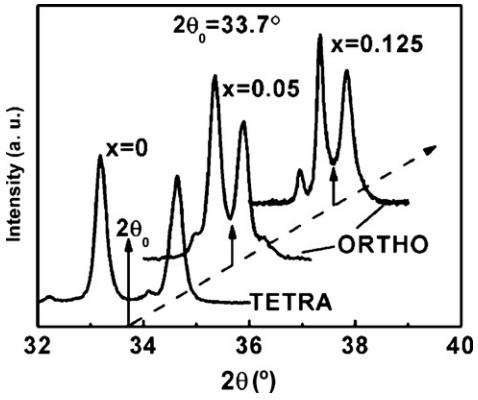

Fig. 3. Portions of XRD patterns ($32° < 2\theta < 36°$) of $Ca_{2-x}Pr_xMnO_4$ compounds ($x = 0$, 0.05 and 0.125) highlighting the Pr-doping effect on the change in the main diffraction peaks. The arrows indicate the angular position $2\theta_0 = 33.7°$.

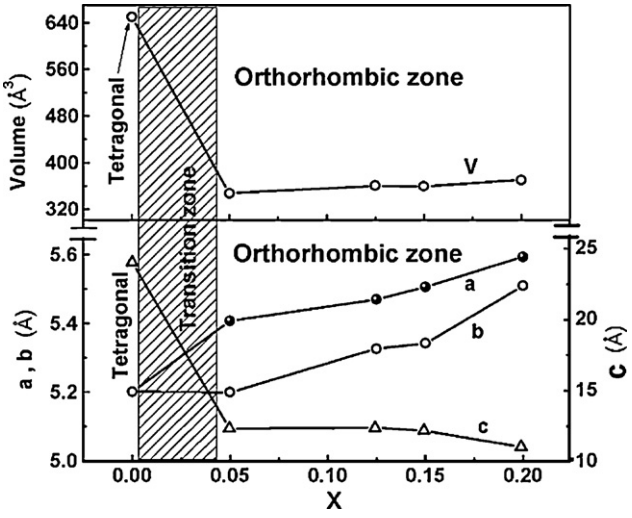

Fig. 4. Composition dependence of cell parameters (a, b and c), and cell volume (V) of $Ca_{2-x}Pr_xMnO_4$ compounds.

Table 1
Cell lattice parameters and volume of $Ca_{2-x}Pr_xMnO_4$ compounds (x = 0–0.2). R_p residuals pattern, R_{wp} Structure factor and χ^2 goodness of fit.

x	Space group	a (Å)	b (Å)	c (Å)	V (Å^3)	χ^2 (%)	R_p (%)	R_{wp} (%)
0	$I4_1/acd$	5.2008(8)	5.2008(8)	24.0433(6)	650	1.94	8.36	13
0.05	Aba2	5.4067(3)	5.1987(1)	12.3494(2)	347	2.16	1.94	2.76
0.125	Aba2	5.4688(2)	5.3258(1)	12.3888(3)	360	1.61	2.74	4.13
0.15	Aba2	5.5053(3)	5.3415(8)	12.1909(1)	359	1.22	3.9	5.00
0.2	Aba2	5.5935(2)	5.5086(8)	11.0331(7)	370	2.92	2.59	4.86

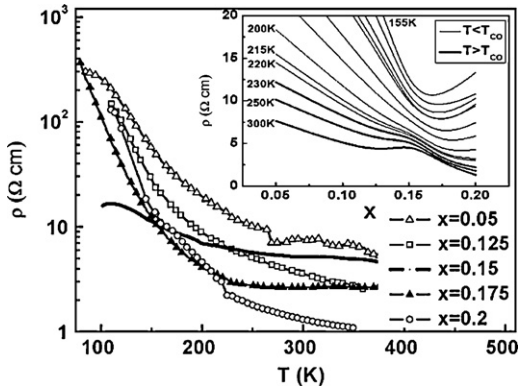

Fig. 5. Resistivity versus temperature for $Ca_{2-x}Pr_xMnO_4$ compounds (x = 0.05–0.2). The inset: isothermal resistivity versus Pr-content.

established orthorhombic zone, a, b and V parameters were found to increase while c parameter decreases.

3.2. Electrical properties

Temperature dependence of dc resistivity $\rho(T)$ for $Ca_{2-x}Pr_xMnO_4$ compounds (x = 0.05–0.2) is presented in Fig. 5. At a given temperature, isothermal resistivity $\rho(x)$, displayed in Fig. 5-inset, exhibits a minimum depending on temperature for x > 0.15. The Pr-substitution in $Ca_{2-x}Pr_xMnO_4$ compounds (initially $Ca_2^{2+}Mn^{4+}O_4^{2-}$ for x = 0) leads to the appearance of a ferromagnetic phase at $T < T_C$ [15,18]. Such behavior is induced by Mn^{3+}–O–Mn^{4+} systems having a ferromagnetic (FM) coupling [19,23]. As known, in both $A_{1-x}B_xMnO_3$ and $A_{2-x}B_xMnO_4$ manganite materials, the substitution of a divalent A-ion by a trivalent B-ion induces a mixed valence Mn^{3+}/Mn^{4+}, enhancing the conduction by e_g electrons hopping through Mn^{3+}–O–Mn^{4+} system [26,27]. Such physical phenomenon, called double exchange (DE), is proved by Zener [28] and used by several authors to explain

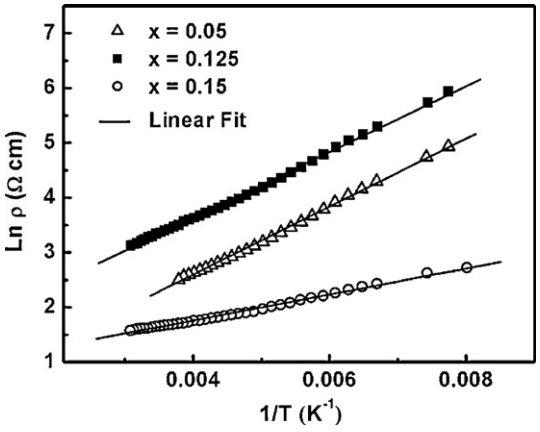

Fig. 6. Logarithmic resistivity versus inverse temperature for $Ca_{2-x}Pr_xMnO_4$ (x = 0.05, 0.125 and 0.15) compounds.

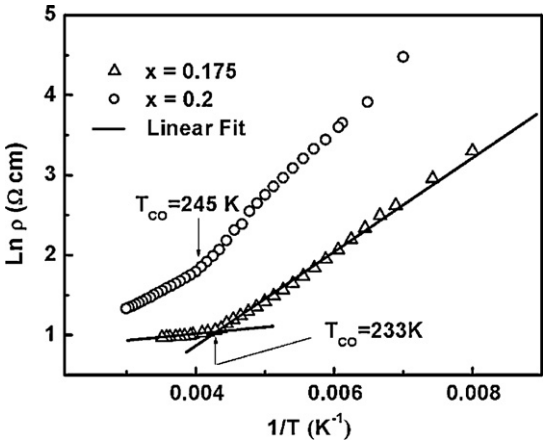

Fig. 7. Logarithmic resistivity versus inverse temperature for $Ca_{2-x}Pr_xMnO_4$ (x = 0.175 and 0.2) compounds.

the electrical transport and the magnetic properties in doped manganites.

From Fig. 5-inset, we can conclude that, for high x-values, as reported in our previous work [23], local antiferromagnetic (AFM) interactions, induced by higher Pr-content, become important and compete with the long-range FM from the DE interactions between Mn ions. Thus, the dc resistivity versus Pr-doping content $\rho(x)$ undergoes an increase. This increase, more important at lower temperatures, can be interpreted by the localization of the conduction electrons and the AFM interactions rise. For lower Pr-content, the $\rho(x)$ decrease is the result of the DE increase characterized by a FM state. Further interpretation details are given later in this section. As known, the semiconductor behavior involves that the charge transport occurs via thermally activated hopping of small polarons [29]. To confirm that, we verify that ρ(T) variation follows the law: $\rho = \rho_0 e^{E_a/kT}$, where E_a is the hopping activation energy. As seen in

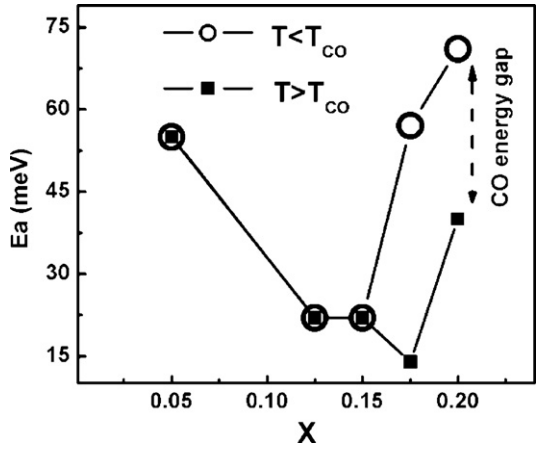

Fig. 8. Hopping activation energy versus Pr-doping content for $Ca_{2-x}Pr_xMnO_4$ (x = 0.175 and 0.2) compounds.

Table 2
Charge-ordering temperature and activation energy of $Ca_{2-x}Pr_xMnO_4$ compounds ($x = 0.05$–0.2).

x	0.05	0.125	0.15		0.175	0.2
T_{CO} (K)	No (CO)			Dc measurements	233	245
				(Ac measurements)	(235)	(248)
E_a (meV)	55	22	22	E_a ($T < T_{CO}$)	57	71
				E_a ($T > T_{CO}$)	14	40

Fig. 6, for $x = 0.05$, 0.125 and 0.15 samples, Ln ρ ($1/T$) curves show a linear variation (Ln $\rho = AT^{-1} + B$) with unique A-slope for each one. E_a is calculated from the slope as $E_a = Ak$, deduced from the linear fit of curves. For $x \geq 0.175$, Ln $\rho(1/T)$ curves (Fig. 7) are fitted by two different straight lines where each one corresponds to a certain temperature range. Thus, the hopping activation energy undergoes an abrupt change (Fig. 8) with an energy gap of about 43 and 31 meV for $x = 0.175$ and 0.2, respectively. This can be interpreted by the presence of a charge-ordering (CO) transition at T_{CO} depending on Pr-doping content [22]. Such charge-ordering is a consequence of the modification of electronic state due to the correlation between the charge carriers of Mn (3d) electrons [30], which point out to the strong competition between FM double exchange interactions, AFM super exchange interactions and the spin–phonon coupling [31]. The augmentation of Mn^{3+} content increases the average MnO_6 distortion, which leads to the reduction of the one-electron bandwidth and, consequently, causes the rise of the AFM state. From certain Mn^{3+}/Mn^{4+} ratio and temperature (T_{CO}), this AFM super exchange dominates the FM double one, which gives rise to the charge-ordered state. Such behavior has been observed by Sdiri et al. in $La_{0.7}Ca_{0.3}MnO_{3-\delta}$ [32], Lopez and de Lima in $Ca_{0.5}Nd_{0.5}MnO_3$ and $Ca_{0.5}Sm_{0.5}MnO_3$ [33], as well as by Jirak et al. in $Ca_xSr_{0.5-x}$ $Pr_{0.5}MnO_3$ [34]. One can observe that the CO state becomes clearly observable at $x = 0.175$, and T_{CO} increases from 233 K for $x = 0.175$ to 245 K for $x = 0.2$. Table 2 summarizes all T_{CO} and E_a obtained results. For each charge-ordered (CO) compound ($x \geq 0.175$), the lowest E_a-value corresponds to CO domain ($T > T_{CO}$). For $x \leq 0.15$, E_a decreases and reaches a minimum

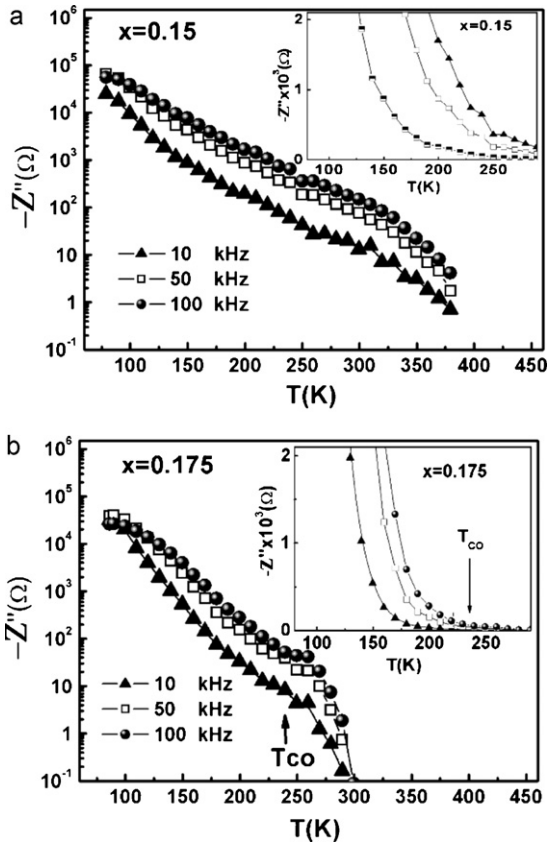

Fig. 9. Temperature dependence of imaginary impedance for $Ca_{2-x}Pr_xMnO_4$ compounds: (a) $x = 0.15$; (b) $x = 0.175$.

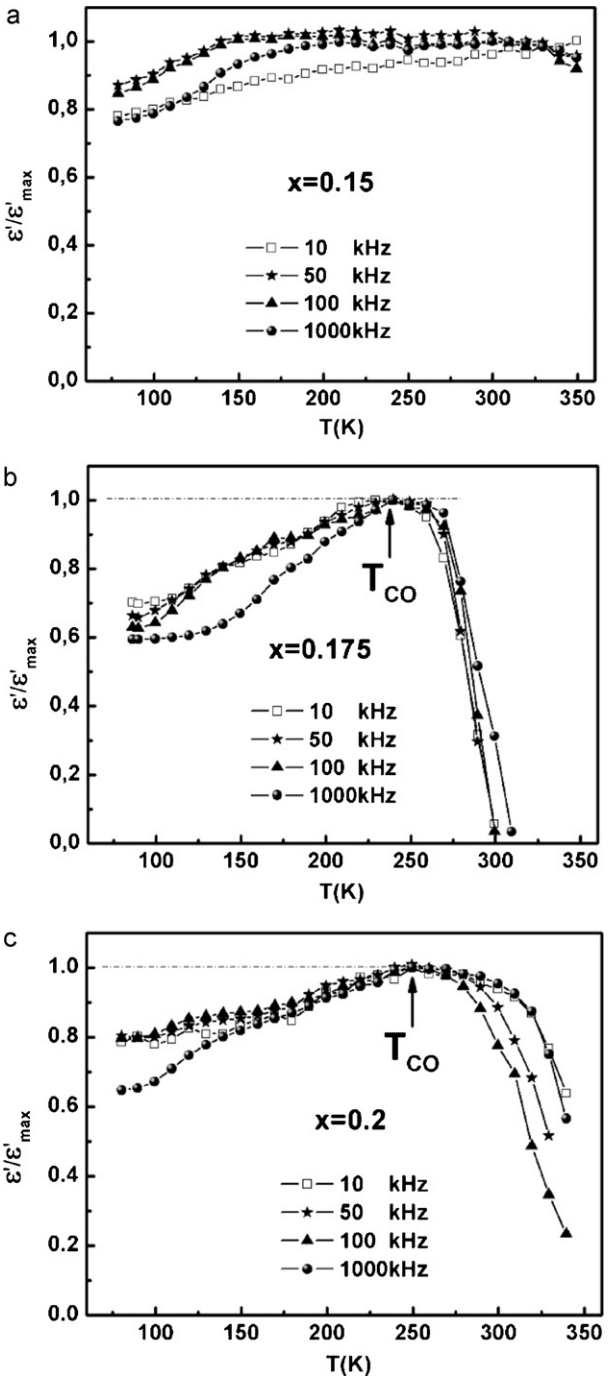

Fig. 10. Temperature dependence of normalized dielectric constant for $Ca_{2-x}Pr_xMnO_4$ compounds: (a) $x = 0.15$; (b) $x = 0.175$; (c) $x = 0.2$.

around $x = 0.15$. This decrease indicates the enhancement of the double exchange (DE) interaction leading to the electrons transfer augmentation between Mn^{3+} and Mn^{4+} ions. The local AFM interactions, induced by the higher Pr-content ($x \geq 0.175$) as mentioned before, explain the E_a increase versus x. Some authors [14,35,36] explain the presence of the CO transition by a complex magnetically frustrated state. Unfortunately, our magnetization measurements M(T) had not been possible at the CO range temperature as shown in the published papers [23,29]. Magnetic measurements made by Rivadulla et al. [14] revealed an additional paramagnetic insulating (PMI) state to the antiferromagnetic insulating (AFI) one. The (PMI-AFI) temperature transition coincides with T_{CO}. This gives evidence of the coupling between the CO state and the AFM behavior.

3.3. Dielectric properties

Fig. 9 represents the temperature dependence of imaginary part of ac electrical impedance $Z''(T)$ at different frequencies. In Fig. 9-b and its inset, it can be seen that, for the CO compound ($x = 0.175$), curves show a quick variation and a frequency splitting taking place when temperature is close to 235 K. This temperature is almost equal to the CO transition temperature deduced from dc resistivity ($T_{CO} = 233$ K). Thus, such compound exhibits capacitive behavior, probably associated to electric dipoles formation enhanced by the CO state. Similar behavior has been observed in $Pr_{0.67}Ca_{0.33}MnO_3$ by Jardón et al. [13] and Rivadulla et al. [14] and in $Ca_{2-x}Pr_xMnO_4$ by Castro-Couceiro et al. [22]. These observations are significantly different from what we find in the non-charge-ordered (NCO) compound ($x = 0.15$), where only a regular monotonous variation is seen in $Z''(T)$ logarithm representation (Fig. 9-a), and a slow variation in the linear representation when temperature is close to T_{CO} (Fig. 9-a-inset). The capacitive behavior accompanying the CO state is confirmed by the representations of the temperature dependence of normalized dielectric constant ($\varepsilon'/\varepsilon'_{max}$) at different frequencies (Fig. 10). For NCO compounds ($x \leq 0.15$), the $\varepsilon'/\varepsilon'_{max}$ variation is very low as shown in (Fig. 10-a) for $x = 0.15$. The CO compounds ($x = 0.175$ and 0.2) indicate a significant $\varepsilon'/\varepsilon'_{max}$ increase (Fig. 10-b and c). Whatever the frequency, each maximum is reached quickly at the same temperature transition (T_{CO}) determined before. For CO compounds, the AF state below T_{CO} minimizes the double exchange between different Mn sites and opposes polaron hopping, which creates electric dipoles [14]. Consequently, the dielectric permittivity increases. So, the CO compounds acquire a strong capacitive response induced by the CO state.

At low temperature ($T < 100$ K), the dielectric permittivity remains constant for a certain temperature range depending on frequency. This phenomenon, which is not the aim of this work, is probably attributed to the existence of a stabilized spin glass state as reported in [23].

4. Conclusions

The sol–gel method was used to synthesis the $Ca_{2-x}Pr_xMnO_4$ compounds. The XRD profiles were indexed with a tetragonal ($I4_1/acd$) structure for Ca_2MnO_4 sample and orthorhombic (Aba2) one for Pr-doped compounds, respectively. The electrical study has revealed a resistivity decrease when temperature increases for low x-values. This was being explained in terms of the double-exchange mechanism importance. The electrical study has showed a semiconductor behavior at high temperature, which has been fitted by the $\rho = \rho_0 e^{E_a/kT}$ law. Resistivity logarithmic representations versus inverse temperature had confirmed the charge-ordering (CO) transition presence for x close to 0.175 at the temperature transition $T_{CO} = 233$ K, which found to be sensitive to Pr-doping content. Each CO compound ($x \geq 0.175$) was found to exhibit a large energy gap, when the temperature reaches T_{CO}-value, which asserts the CO-interactions role in the hopping activation energy variation. At T_{CO}, both dielectric permittivity and imaginary part of ac electrical impedance of CO compounds show a significant increase, highlighting a strong capacitive response.

Acknowledgements

This work, within the frame work of collaboration, is supported by:

- The Tunisian Ministry of Higher Education and Scientific Research.
- The Portuguese Ministry of Science, Technology and Higher Education.
- The French Ministry of Higher Education and Scientific Research.

References

[1] K. Bärner, H. Deng, W. Morsakov, I.V. Medvedev, C.P. Yang, J. Alloys Compd. 500 (2010) 16–21.
[2] H. Yi Liu, C. Kong, Zhu, J. Alloys Compd. 439 (2007) 33–36.
[3] M.T. Tlili, M. Bejar, E. Dhahri, M. Sajieddine, M.A. Valente, E.K. Hlil, J. Mater. Charact. 62 (2011) 243–247.
[4] A. Tozri, E. Dhahri, E.K. Hlil, J. Magn. Magn. Mater. 322 (2010) 2516–2524.
[5] Y. Feng, M. Zhang, J. Magn. Magn. Mater. 322 (2010) 2675–2679.
[6] P.T. Phong, N.V. Dai, D.H. Manh, T.D. Thanh, N.V. Khiem, L.V. Hong, N.X. Phuc, J. Magn. Magn. Mater. 322 (2010) 2737–2741.
[7] S.K. Misra, S.I. Andronenko, S. Asthana, D. Bahadur, J. Magn. Magn. Mater. 322 (2010) 2902–2907.
[8] M. Staruch, L. Stan, F. Ronning, J.D. Thompson, Q.X. Jia, J. Yoon, H. Wang, M. Jain, J. Magn. Magn. Mater. 322 (2010) 2708–2711.
[9] E.J. Verwey, Nature 144 (1939) 327.
[10] S.A. Kivelson, I.P. Bindloss, E. Fradkin, V. Oganesyan, J.M. Tranquada, A. Kapitulnik, C. Howald, Rev. Mod. Phys. 75 (2003) 1201.
[11] J. Linde, P. Karen, J. Solid State Chem. 183 (2010) 2703–2713.
[12] Kong Hui, Zhu Changfei, J. Alloys Compd. 478 (2009) 805–808.
[13] C. Jardón, F. Rivadulla, L.E. Hueso, A. Fondado, A. Rivas, J. López Quintela, R. Zysler, M.T. Causa, P.M.A. Sande, J. Magn. Magn. Mater. 196 (1999) 475.
[14] F. Rivadulla, M.A. López Quintela, L.E. Hueso, C. Jardón, A. Fondado, J. Rivas, M.T. Causa, R.D. Sánchez, Solid State Commun. 110 (1999) 179.
[15] J. Sichelschmidt, M. Paraskevopoulos, M. Brando, R. When, D. Ivannikov, F. Mayr, K. Pucher, J. Hemberger, A. Pimenov, H.A. Krug Von Nidda, P. Lunkenheimer, V.Y. Ivanov, A.A. Mukhin, A.M. Balbashov, A. Loidl, Eur. Phys. J. B 20 (2001) 77.
[16] J. Rivas, B. Rivas-Murias, A. Fondado, J. Mira, M.A. Señarís Rodríguez, Appl. Phys. Lett. 85 (2003) 6224.
[17] S. Yáñez Vilar, A. Castro-Couceiro, B. Rivas-Murias, A. Fondado, J. Mira, J. Rivas, M.A. Señarís-Rodríguez, Z. Anorg. Allg. Chem. 631 (2005) 2265.
[18] A. Castro-Couceiro, S. Yáñez Vilar, B. Rivas-Murias, A. Fondado, J. Mira, J. Rivas, M.A. Señarís-Rodríguez, J. Phys. Condens. Matter 18 (2006) 3803.
[19] J.L. Cohn, M. Peterca, J.J. Neumeier, Phys. Rev. B 70 (2004) 21433.
[20] J.L. Cohn, M. Peterca, J.J. Neumeier, J. Appl. Phys. 97 (2005) 034102.
[21] F. Lichtenberg, A. Herrnberger, K. Wiedenmann, Prog. Solid State Chem. 36 (2008) 253–387.
[22] A. Castro-Couceiro, M. Sánchez-Andújar, B. Rivas-Murias, J. Mira, J. Ivas, M.A. Señarís-Rodríguez, Solid State Sci. 7 (2005) 905.
[23] M.T. Tlili, M. Bejar, E. Dhahri, M.A. Valente, L.C. Costa, E.K. Hlil, Open Surf. Sci. J. 1 (2009) 54.
[24] J. Takahashi, N. Kamegashira, Mater. Res. Bull. 28 (1993) 451–460.
[25] A. Daoudi, G. Le Flem, J. Solid State Chem. 5 (1972) 57.
[26] A.M. Haghiri-Gosnet, J.P. Renard, J. Phys. D: Appl. Phys. 36 (2003) 127.
[27] W. Boujelben, M. Ellouze, A. Cheikh-Rouhou, J. Pierre, Q. Cai, W.B. Yelo, K. Shimizu, C. Dubourdieu, J. Alloys Compd. 334 (2002) 1.
[28] C. Zener, Phys. Rev. 82 (3) (1951) 403.
[29] M. Ibarra, R. Retoux, M. Hervieu, C. Autret, A. Maignan, C. Martin, B. Raveau, J. Solid State Chem. 170 (2003) 361.
[30] K. Kitamoto, K. Ichikawa, K. Mimura, O. Aita, S. Kawamata, T. Ishida, Y. Taguchi, Electron. Struct. Condens. Matter 19 (B) (2001) 6011.
[31] J. Lopez, P.N. Lisboa Filho, W.A.C. Passos, W.A. Ortiz, F.M. Araujo-Moreira, K. Ghosh, D. Schaniel, O.F. De Lima, Phys. Rev. B 63 (22) (2001) 224422.
[32] N. Sdiri, M. Bejar, E. Dhahri, J. Magn. Magn. Mater. 311 (2007) 512–516.
[33] J. Lopez, O.F. De Lima, J. Alloys Compd. 369 (2004) 227.
[34] Z. Jirak, F. Damay, M. Hervieu, C. Martin, B. Raveau, G. André, F. Bourée, Phys. Rev. B 61 (2000) 1181.
[35] H. Yoshizawa, H. Kawano, Y. Tomioka, Y. Tokuram, Phys. Rev. B 52 (1995) 13145.
[36] A. Maignan, C. Martin, F. Damay, B. Raveau, Z. Phys. B: Condens. Matter 104 (1997) 21.